Food Chemistry: X 25 (2025) 102189

Contents lists available at ScienceDirect

Food Chemistry: X

journal homepage: www.sciencedirect.com/journal/food-chemistry-x

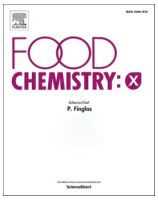

Harmonious regulation flavor and lipid oxidation in dry-cured tenderloin through electrical stimulation: A study on lipase activity and sensory correlations

Lisha Lan, Li Chen, Xiaolin Zhong, Weiguo Cao, Ying Zhou, Jing Wan, Yuanyuan Liu, Qinjin Zhu *

Guizhou Key Laboratory of New Quality Processing and Storage of Ecological Specialty Food, School of Liquor and Food Engineering, Guizhou University, Guiyang 550025, China

ARTICLE INFO

Keywords:
Dry-cured tenderloin
Electrical stimulation
Lipid oxidation
GC–MS
Flavor component

ABSTRACT

This study examined the effects of electrical stimulation on dry-cured tenderloin at different processing stages (0, 4, and 11 days), with a primary focus on lipid oxidation and the composition of volatile compounds. The study's results revealed that electrical stimulation enhanced lipase activity and accelerated lipid oxidation. Compared to the control group, the electrically stimulated samples exhibited higher total amino acid and fatty acid contents. Furthermore, the electrically stimulated group demonstrated superior taste (as assessed by an electronic tongue) and aroma profiles (as assessed by an electronic nose). Among the 49 compounds identified by GC–MS, the electrically stimulated dry-cured tenderloin displayed a greater diversity of volatile compounds. Notably, certain compounds, including ethyl lactate, ethyl myristate, 2,3-octanedione, and cyclohexanone, were exclusively detected in the electrically stimulated samples. These findings offer novel insights into the interplay between lipid oxidation and flavor development during meat processing via electrical stimulation.

1. Introduction

Dry-cured tenderloin is one of the classics of traditional Chinese cured products and is also a good source of nutrients such as lipids and proteins (Fu et al., 2022).

Flavor was identified as a principal characteristic of dry-cured tenderloin throughout the dry curing process. Lipid metabolism was recognized as a principal pathway contributing to flavor development. During the curing process of dry-cured tenderloin, lipases were classified as a group of enzymes that played a key role in enhancing flavor. Lipases, which include acid lipases, neutral lipases, and phospholipases, are a class of enzymes characterized by a catalytic triad composed of serine, histidine, and either aspartic or glutamic acid residues (Chaves Almeida et al., 2023). These enzymes, in conjunction with lipoxygenases (LOX), facilitate the hydrolysis of lipids. The primary function of lipase was to facilitate the hydrolysis of lipids. Triglycerides and phospholipids were hydrolyzed by lipase, yielding fatty acids and additional hydrolysis byproducts. Fatty acids were oxidized to produce hydroperoxides, which subsequently underwent further oxidation to generate aldehydes, ketones, esters, and an array of volatile compounds, and it was these volatile flavor compounds that constituted the principal contributors to the flavor profile (Guo et al., 2019).

At present, techniques such as high-pressure processing, microwave, and ultrasonication have been suggested for the enhancement and stabilization of enzymatic activity. There were also investigations aimed at augmenting lipase activity through the immobilization of the enzyme, enhancement of the enzyme's active site, and the application of ionic liquids as intervention agents (Dias et al., 2018). However, the widespread utilization of these technologies was constrained by a multitude of factors. Electrical stimulation (ES) offers several advantages over alternative techniques, including its widespread application, environmental sustainability, and safety. Furthermore, it enhances the tenderness and colour of tenderloin. Originally, ES was employed as a physical method of slaughter, intended to induce muscle contraction by passing an electric current through the body or carcass of a freshly slaughtered animal, thereby accelerating the rate of glycolysis and resulting in a decrease in pH (Hwang et al., 2003). Current intensity, voltage, duration, and frequency are key parameters influencing tenderloin quality

* Corresponding author.
E-mail address: ls.qjzhu@gzu.edu.cn (Q. Zhu).

https://doi.org/10.1016/j.fochx.2025.102189
Received 27 November 2024; Received in revised form 5 January 2025; Accepted 13 January 2025
Available online 16 January 2025

through ES. The ES is classified into three categories based on the voltage intensity: ultra-low voltage ES (below 45 V), low-voltage ES (45–100 V), and high-voltage ES (100–500 V) (Zhang et al., 2019). In recent studies, it was demonstrated that ES enhanced the activities of histone proteases B and L and accelerated protein degradation (Zhang et al., 2024). Furthermore, ES was found to enhance the tenderness and flavor of beef, concurrently diminishing off-flavors such as blood and slurry. It also diminishes the Neu5Gc content in red meat, improving health quality (Xu et al., 2022), and degrades myofibrillar proteins during processing.

However, the influence of ES on lipase activity and the flavor profile throughout the processing of dry-cured tenderloin has remained underexplored. In this study, tenderloins underwent ES at different processing stages to assess the impact of ES on pork cell integrity, the activity of lipoxygenase and three distinct lipases, and the level of lipid oxidation, as indicated by malondialdehyde (MDA) and peroxide value (POV) levels. The alterations in amino acid and fatty acid profiles were monitored. Concurrently, electronic tongue, electronic nose, and gas chromatography–mass spectrometry (GC–MS) analyses were employed to investigate the influence of ES on the taste and aroma profiles of dry-cured tenderloin.

2. Materials and methods

2.1. Dry cured tenderloin processing

The pork tenderloin used in the experiment was provided by Guizhou Tainong Xingwang Food Co. Ltd. (Huimin Fresh Supermarket, Huaxi District, Guiyang City, China), which was controlled within 6 h from slaughter to purchase and processed within 12 h. It was split into (15 ± 1.5) cm × (7 ± 1) cm × (5 ± 1) cm sized tenderloin pieces in the laboratory. The conductive aluminium plates were then placed vertically, and the tenderloin was placed in the direction of fibre between the two conductive aluminium plates. The groupings of the ES treatments are shown in Table 1. In our experiments, the parameters of the ES that we applied were as follows: a variable AC power (AFV-P600, Preen Power Supply Co., Ltd., Suzhou, China) supply with a current of 0.7 A, a duration of 90 s, and a voltage range of 15–40 V, which we classified as low-voltage ES. The specific experimental groupings and treatments are shown in Table 1. The experimental groups were defined as follows: CK (no electrical stimulation), 0-ES (electrical stimulation at 0 days), 4-ES (electrical stimulation at 4 days), and 11-ES (electrical stimulation at 11 days).

The preparation of dry-cured tenderloins consisted of five different sampling stages: day 1 (1 day of salt curing at 4 °C using 2 % of the sample weight of salt evenly kneaded and vacuum-sealed), day 5 (5 days of salt curing at 4 °C using 2 % of the sample weight of salt evenly kneaded and vacuum-sealed), day 12 (7 days of drying at 8 °C and 80 % relative humidity in an incubator after salt curing), day 20 (8 days of pre-ripening at 15 °C and 70 % relative humidity), and day 30 (tenderloin continues to end-ripening for 10 days).

2.2. Salt content and hematoxylin-eosin (HE) staining

Weigh the sample (1 g) and add 10 times the volume of distilled water and homogenize at 4000 revolutions per min (Homogenizer belongs to XHF-D, Ningbo Xinzhi Biotechnology Co) for 1 min (Contreras-Lopez et al., 2020). The homogenate was then measured using a digital salinometer (model ES-421). The obtained salinity value was multiplied by 10 to convert it into the salt percentage.

$$\text{Salt percentage} = \text{Salinity value} \times 10 \quad (1)$$

where: The salinity value indicates the number displayed by the salinometer.

Sections were prepared from samples at 4 μm thickness using a microtome. After deparaffinization, they were stained with Harris hematoxylin for 8 min, then differentiated in 1 % hydrochloride alcohol for a few seconds, and blued with 0.6 % ammonia. The sections were subsequently washed, stained with eosin for 3 min, dehydrated, and sealed with neutral gum. Finally, to facilitate the clear observation and subsequent documentation of tissue structure and cellular morphology, the pre-treated samples were carefully mounted on microscope slides and imaged using a microscope equipped with a digital camera for high-resolution documentation (Yue et al., 2024).

2.3. Lipid oxidation

2.3.1. Malondialdehyde (MDA) values

The sample (0.1 g) was weighed and 1 mL of extraction solution was added, then homogenized on ice for 1 min at 8000 revolutions per min. Subsequently, the samples were centrifuged (GTR16–2 Benchtop High-Speed Refrigerated Centrifuge, Beijing Beili Times Medical Technology Co) at 8000 rmp for 10 min at 4 °C, and the supernatant was immediately placed on ice for subsequent testing. Protein concentration was measured by using a BCA assay kit (Beijing Solarbio Science & Technology Co.,Ltd.). The MDA content was measured by using a MDA assay kit (Beijing Solarbio Science & Technology Co.,Ltd.).

$$\text{MDA(nmol/mg prot)} = 53.763 \times \Delta A \div \text{Cpr} \times F \quad (2)$$

where: The difference in absorbance $\Delta A = \Delta A_{532} - \Delta A_{600}$; Cpr denotes the protein concentration of the sample, mg/mL; F denotes the dilution of the sample solution.

2.3.2. Peroxide value

0.5 g of the sample was dissolved by 10 mL of phosphate buffer (40 mM, pH 6.8), homogenized, and then 10 mL of chloroform-methanol (7:3, *v*/v) was added and mixed homogeneously. 50 μL of ammonium thiocyanate solution (at 3 % concentration) and 50 μL of ferrous iron(II) solution were added to the reaction system for 10 min before centrifuging the reaction for 10 min (3000 rmp, 4 °C) and the absorbance of the sample was measured at 500 nm (Cao et al., 2019). The absorbance of the samples was determined. The results were expressed as milli-equivalent (meq) of lipid peroxides per kilogram.

$$\text{POV(meq/kg)} = \frac{[(As - \text{Ab}) \times \text{M}]}{55.84 \times \text{m} \times 2} \quad (3)$$

where: As denotes the absorbance of the sample; Ab denotes the absorbance of the blank control group; M = 41.52; m = mass of the sample; 55.84 denotes the atomic weight of iron.

2.4. Lipoxygenase (LOX) activity

After homogenising 2.5 g of sample with 10 mL of saline, the supernatant was taken and filtered after centrifugation for 10 min (10,000 rmp, 4 °C) (Guo et al., 2019). The protein concentration was also determined. The enzyme reaction system consisted of 20 μL of supernatant, 20 μL of linoleic acid substrate and 160 μL of sodium citrate buffer solution (50 mmol/L, pH 5.5), and the increase in absorbance at 234 nm for 1 min was determined. An increase in OD of 0.001 represented one unit of enzyme viability (U), and the treatment group without enzyme solution served as the control group.

Table 1
The application of electrical stimulation at different stages of the processing period.

Group	ES treatment	Electric current (A)	Time(s)	Sampling time(day)
CK	control	0	0	1 , 5 , 12 , 20 , 30
0-ES	0 day	0.7	90	
4-ES	4 day	0.7	90	
11-ES	11 day	0.7	90	

$$\text{LOX activity(U)} = \frac{(A_{1\ min} - A_{0\ min}) - A_{control}}{0.001} \quad (4)$$

where: $A_{1\ min}$ indicates the absorbance at 234 nm after 1 min of reaction.; $A_{0\ min}$ indicates the absorbance at 234 nm without reaction.; $A_{control}$ indicates the absorbance at 234 nm for the control group.

2.5. Lipohydrolase activity

A 1 g sample should be accurately weighed and combined with 15 mL of lysis buffer containing 5 mM EGTA and 50 mM phosphate at a pH of 7.5 (Ripolles et al., 2011). The mixture should be homogenized under ice bath conditions followed by centrifugation at 10,000 rpm for 20 min at 4 °C. The precipitate should be discarded, and the supernatant should be collected and set aside. The protein concentration in the crude enzyme solution should then be determined.

2.5.1. Acid lipase

The initial reaction system consisted of 10 μL of crude enzyme solution, 280 μL of reaction buffer (consisting of 0.05 % (*w/v*) Triton X-100, 0.1 M disodium phosphate (pH 5.0), 0.05 M citrate buffer, and 0.8 mg/mL (pH 5.0) bovine serum albumin (BSA)), and 10 μL of substrate (1 mM 4-methylumbelliferyl oleate), and the reaction was terminated by adding 10 μL of HCl (1 M) after incubation at 37 °C for 30 min. The excitation wavelength was 350 nm and the emission wavelength was 445 nm.

2.5.2. Neutral lipase

The reaction system consisted of 10 μL of crude enzyme solution, 280 μL of reaction buffer (consisting of Tris/HCl, 0.22 M, pH 7.5) and 10 μL of substrate, which were mixed well and incubated at 37 °C for 30 min to detect the fluorescence, and the excitation wavelength was 350 nm and the emission wavelength was 445 nm.

2.5.3. Phospholipase

The initial reaction system consisted of 10 μL of crude enzyme solution, 280 μL of reaction buffer (consisting of (0.05 %, *w/v*) Triton X-100, 0.1 M disodium phosphate (pH 5.0), 0.05 M citrate buffer, 0.8 mg/mL (pH 5.0) bovine serum albumin (BSA), and 150 mM sodium fluoride), and 10 μL of substrate, and was incubated for 30 min at 37 °C. After incubation for 30 min, the reaction was terminated by adding 10 μL of HCl (1 M). The excitation wavelength was 350 nm and the emission wavelength was 445 nm.

2.6. Amino acid

For the extraction of a 1 g sample, 50 mL of 0.01 mol/L hydrochloric acid was employed, with the procedure conducted for a duration of 30 min (Zhang et al., 2024). The solution was filtered, and subsequently, 2 mL of the filtrate was collected and mixed with an equal volume of 8 % sulfosalicylic acid. Following centrifugation at 10,000 rpm for 10 min at 4 °C, the supernatant was passed through a membrane filter. The resulting filtrate was then reserved for subsequent analysis. A fully automated amino acid analyzer model S—433D (Secam, Germany) was used. Identification and quantification of amino acids were conducted utilizing standard amino acids mixtures of type H from WAKO. The results were reported as milligrams per 100 g of muscle tissue.

2.7. Fatty acid

Weigh 60.0 mg of sample into a stoppered test tube and add 2.0 mL of internal standard solution (undecanoic acid triglyceride: $C_{36}H_{68}O_6$). Fatty acid methyl esters (FAMEs) were prepared by dissolving the sample in a test tube with 4 mL of isooctane. Once dissolved, 200 μL of potassium hydroxide-methanol solution was added and the mixture was shaken for 30 s and allowed to stand until clarified. Approximately 1 g of sodium bisulfate was added to neutralize the potassium hydroxide. After the salt precipitation had been completed, the upper solution was stored for determination. FAMEs analysis was conducted using an Agilent 7020 A gas chromatograph equipped with a flame ionization detector (Chen et al., 2024). The injector and detector temperatures were set to 270 °C and 280 °C, respectively. A highly polar stationary phase of dicyanopropyl siloxane chromatographic column (100 m length, 0.25 mm inner diameter, 0.2 μm film thickness) was used. The temperature program was as follows: initial temperature 100 °C for 13 min; 100 °C to 180 °C at 10 °C/min, held for 6 min; 180 °C to 200 °C at 1 °C/min, maintained for 20 min; 200 °C to 230 °C at 4 °C/min, maintained for 10.5 min. The sample size was 1.0 μL, nitrogen was used as the carrier gas, and the split ratio was 100:1. The fatty acid content was calculated by determining the corresponding peak area as a percentage of the total peak area of all components.

2.8. E-tongue

Chopped dry-cured tenderloins (10 g) was mixed with 90 mL of distilled water at 40 °C and homogenized for 1 min (Du et al., 2021). The resulting solution was filtered through gauze, followed by centrifugation at 3000 rpm for 10 min at 4 °C. Then 60 mL of the supernatant was taken and analyzed for flavor using an electronic tongue instrument (Model: SA402B, INSENT CO., LTD.) equipped with a professional probe. The control solution was 0.3 mM tartaric acid and 30 mM potassium chloride. The analysis was carried out using a two-step cleaning method, with a positive cleaning solution of 10 mM potassium hydroxide, 100 mM potassium chloride and 30 % volume ethanol, and a negative cleaning solution of 100 mM hydrochloric acid and 30 % volume ethanol. The electrical signal data were converted to taste values for subsequent data analysis using the taste analysis software included with the instrument.

2.9. E-nose

Chopped dry-cured tenderloins (3 g) were accurately weighed and transferred to 20 mL Agilent DK2001 headspace vials (Du et al., 2021). The bottle was sealed with a cap with a white silicone gasket. The headspace vials were heated in a water bath at 50 °C for 10 min in order to stimulate the aroma of the samples. Measurements were performed with the Airsense PEN3 electronic nose: cleaning time of 100 s, measurement time of 240 s, sensor flow rate of 150 mL/min and measurement sample flow rate of 100 mL/min. The data obtained were used for analysis after primary processing using the data processing software (WinMuster) that comes with the electronic nose instrument. The response characteristics of each sensor of the electronic nose are shown in Table S1.

2.10. Volatile organic compounds (VOCs)

Volatile compounds were identified by gas chromatography–mass spectrometry (GC–MS) according to the method described in previous studies (Liu et al., 2022). Solid phase microextraction (SPME) was used to pre-treat the samples. The sample (1 g) was accurately weighed into a 20 mL headspace vial, 10 μL of internal standard (sec-octanol, Aladdin) was added, and the sample was incubated for 10 min at 80 °C. The pre-treated SPME extraction head (57329-U, DVB/CAR/PDMS, Supelco) was transferred to the incubation chamber and the sample was adsorbed for 25 min at 80 °C. After adsorption, the SPME extraction head was transferred to the GC injection port (8890 A, Agilent Technologies, Palo Alto, CA, USA) and desorbed for 5 min at 250 °C. After injection, the SPME extraction head was aged for 10 min at 270 °C. 10 μL of n-alkanes (1000 mg/L, SIGMA) was taken into a 20 mL headspace vial, incubated for extraction, and injected. Gas-phase conditions: A DB-Heavy Wax column (30 m × 250 μm × 0.5 μm) was utilized, with high-purity helium serving as the carrier gas at a constant flow rate of 1.0 mL/min. The

initial column temperature was maintained at 50 °C for 2 min, followed by a linear temperature ramp to 230 °C at a rate of 5 °C/min, where it was held for an additional 5 min. Mass spectrometry conditions (LECO, Pegasus BT 4D): The mass spectrometry transmission line was set at 250 °C, the ion source at 250 °C, with an acquisition rate of 10 spectra per second. The electron bombardment energy was 70 eV, the detector voltage was set to 2014 V, and the mass spectrometry scan range was from m/z 35 to 550. The volatile compounds were identified using information such as mass spectra, linear retention time and peak area. The data were area normalised in order to allow comparison of different data.

2.11. Statistical analysis

The results are presented as the mean ± standard deviation, derived from a minimum of three independent samples. Statistically significant differences among groups ($p < 0.05$) were ascertained utilizing Duncan's multiple range test following analysis of variance (ANOVA), conducted with IBM SPSS Statistics 27 software (SPSS, Inc., Chicago, Illinois, USA). All graphs were plotted using Origin 2022 software. Additionally, data analysis and plotting of data from the e-nose were performed using the specialized software WinMuster.

3. Results and discussion

3.1. Salt content and HE staining in dry-cured tenderloins

Salting is a critical process in the preparation of dry-cured tenderloin, and the flavor of the final product is affected by it. Fig. 1A illustrates that the salt content in both the CK and ES groups rose steadily over processing time, peaking at the end. This is due to the salt particles on the outside of the tenderloin during the curing process resulting in excessive salt concentration and generating internal and external osmotic pressure. The liquid solution inside the cells exudes and dissolves the external salt and forms a salt solution, which enters the tenderloin resulting in a rapid increase in salt content. The ES group had a faster rise in salt content due to the electric shock that penetrates the cells and facilitates the rate of diffusion. Prior research has demonstrated that the overall palatability of ham is enhanced with an increase in salt content (Lorido et al., 2015).

HE staining revealed tissue cell changes after various treatments. Notably, 2 % salt pickling (Fig. 2B) and ES (Fig. 2E) alone led to more cell damage than fresh meat (Fig. 2A and D). The most significant effect was seen with combined 2 % salt and ES treatment, particularly after 4 days of marination followed by ES (Fig. 2F), confirming higher salt levels in the 4-ES group. Previous research showed that during curing, water from the tenderloin dissolved the dry salt, creating a solution that could damage muscle cells (Martuscelli et al., 2017). The 4-ES group's higher salt content is believed to result from ES applied during the curing process. This method also allowed salt molecules in the muscle tissue to diffuse towards the center, speeding up the release of lipase enzymes involved in flavor development.

3.2. Lipid oxidation products in dry-cured tenderloins

Fig. 1B illustrated the changes in MDA content, a key biomarker of lipid oxidation, during the processing period. The trend in MDA content exhibited an initial increase followed by a gradual decrease after day 12. The initial increase in MDA content was attributed to the accumulation of aldehydes, which were oxidation byproducts of fatty acids in meat. MDA content peaked on day 12, with levels of 0.38, 0.44, 0.50, and 0.43 nmol/mg in the CK, 0-ES, 4-ES, and 11-ES groups, respectively. The MDA values in the three ES-treated groups were significantly higher than those of the CK group, suggesting an accelerative effect of ES on MDA production. ES treatment enhanced MDA formation by disrupting cell membrane integrity and promoting pro-oxidative lipid interactions and oxidative reactions (Ma et al., 2007). Studies report that MDA levels exceeding 1.0 mg/kg are deemed unacceptable due to their potential to cause spoilage odors in meat. However, during the processing of dry-cured tenderloin, the peak MDA was well below this threshold, so ES treatment did not negatively affect flavor. The slight decrease in MDA levels observed at days 20 and 30 was attributed to the degradation of unstable MDA into volatile compounds, or its interaction with the free amino acid groups of proteins (Karabagias et al., 2011).

POV, a key flavor precursor arising from initial lipid oxidation, is prone to further oxidation, yielding aldehydes, ketones, and other compounds. ES facilitated this process during the early stages of dry-cured loin processing when the oils and fats began to oxidize in the presence of oxygen, generating progressively higher levels of peroxides and therefore a consequent increase in POV values. The POV value exhibited a biphasic change, peaking at 12 days with maximum values of 0.0042, 0.0061, 0.0072, and 0.0064 meq/kg for the CK, 0-ES, 4-ES, and 11-ES groups, respectively (Fig. 1C). Notably, the 4-ES group showed the highest POV value. Despite ES-induced increases in POV, these values remained well below the safety threshold for dry-cured ham (0.25 g/100 g fat), ensuring human consumption safety (Fernandez et al., 2020). Combined with the results of HE cell staining, it was inferred that the 4-ES group, which exhibited the highest degree of cell disruption (Fig. 2F), led to increased oxidation due to increased contact between oxygen and tissue. The POV value then decreased gradually, likely due to the acceleration of the decomposition rate of peroxide, which was attributed to the change in fermentation temperature at that time.

3.3. LOX activity in dry-cured tenderloins

LOX, a class of dioxygenases, is capable of promoting lipid oxidation and catalyzing the oxidation of fatty acids to yield volatile flavor compounds. The activation process of LOX is closely related to the form of iron ions present (Lapenna et al., 2009). The results of the experiment showed that there was no significant difference in LOX activity between the groups at 1 day. As observed from 5 day (Fig. 1D), the LOX activity of both 0-ES and 4-ES groups was stronger than that of CK group ($p < 0.05$) and higher than that of 1 day, and LOX of 4-ES group showed a stronger activity (22.0 U/g protein). This phenomenon was observed because the salt had penetrated into the substrate following the completion of the pickling, catalyzing the production of a portion of hydroperoxides, which induced the conversion of Fe^{2+} to Fe^{3+}, and resulted in the activation of the LOX (Lapenna et al., 2009). The ES treatment is performed after 4 days of curing. ES electroporates intact cells that have not yet been damaged by salt, destroying the lysosomes in the cells and accelerating the release of small peptides with activating effects. At 12 day, LOX viability was the highest in all groups, and the 11-ES group also showed an increase in enzyme viability, indicating that ES can effectively promote LOX viability in cells. The significant decrease in LOX activity observed between the 20 day and 30 day of ripening may be attributed to the loss of water associated with processing, which results in an increased salt content and disruption of the LOX structure (Hu et al., 2023). Alternatively, the proteases released due to cellular disruption could also exert a destructive effect on LOX.

3.4. Lipohydrolase activity in dry-cured tenderloins

Lipases are usually divided into three categories based on their activity: acid lipases, neutral lipases, and phospholipases. Acid lipases are typically localized in lysosomes, while neutral lipases and phospholipases are predominantly found in adipose tissue. The enzymatic activity of lipases is modulated by their specific cellular locations. After ES at different processing stages, the activities of the three fat hydrolases followed a similar trend, increasing and then decreasing during the processing period, with the difference that acid lipase and phospholipase reached their maximum values at 5 day, with maximum enzyme activities of 7.36 U/g protein and 4.99 U/g protein, respectively,

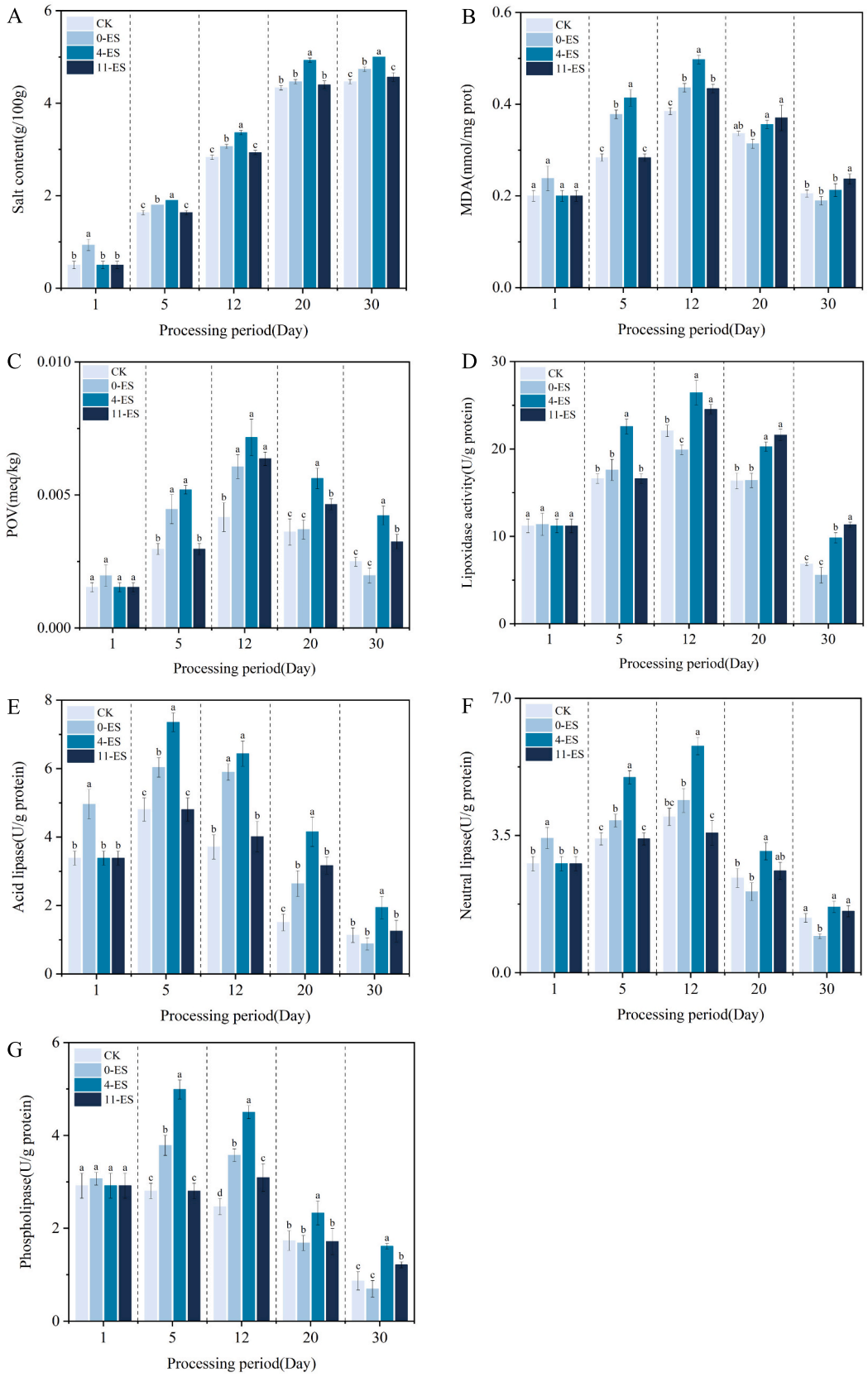

Fig. 1. Salt content (A); MDA (B); POV (C); LOX (D); acid lipase (E); neutral lipase (F) and phospholipase (G) of dry-cured tenderloins after ES at different processing periods. Different lower case letters in the graphs indicate significant differences between samples at different fermentation times ($p<0.05$).

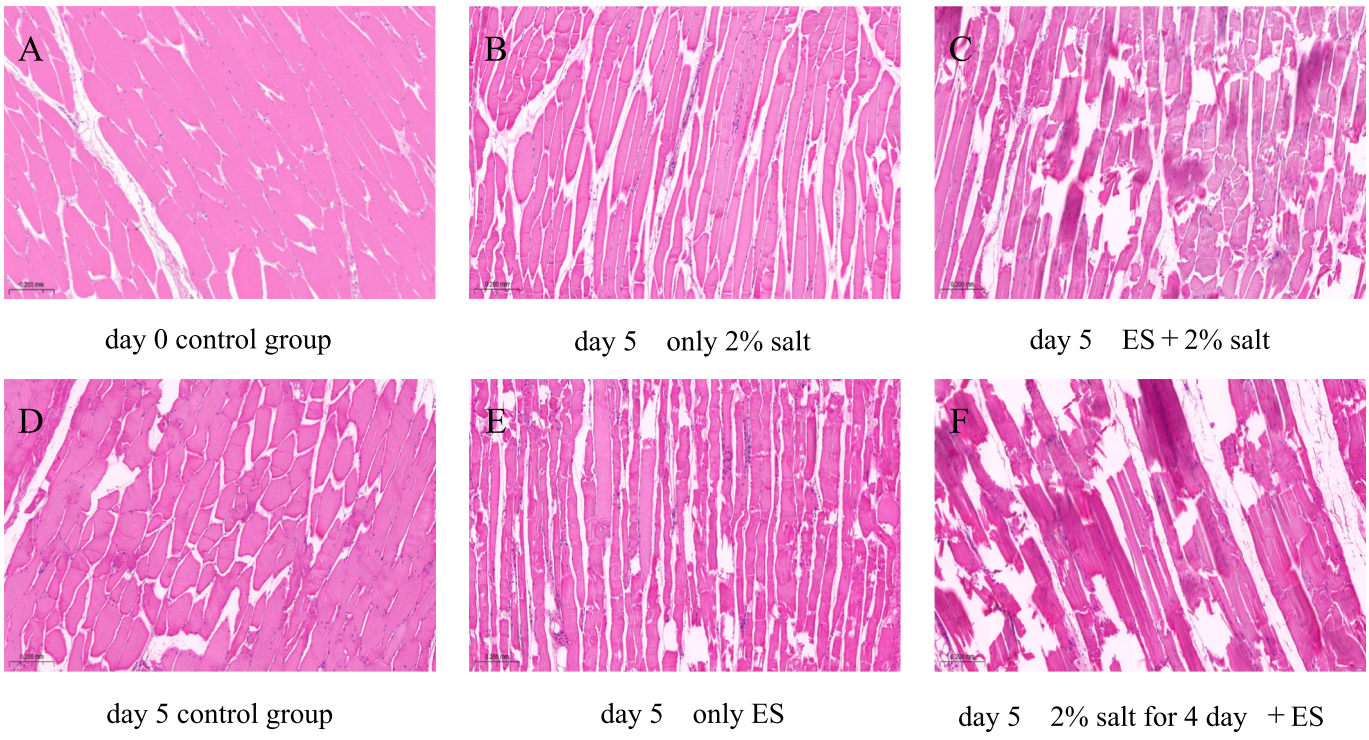

Fig. 2. HE staining of samples under each treatment: (A) 0 day of fresh meat; (B) marinated with 2 % salt only for 5 day; (C) subjected to ES and then marinated with 2 % salt for 5 day; (D) 5 day of fresh meat; (E) treated with ES only and then left for 5 day; and (F) marinated with 2 % salt for 4 day and then subjected to ES.

whereas neutral lipase reached its maximum value at 12 day (3.10 U/g protein). ES treatment increased acid lipase activity (Fig. 1E), with the 4-ES group showing a 53 %, 73 %, 176 %, and 72 % increase in activity over the control group at each processing period except the 1 day, respectively. This is because ES not only disrupts the lysosomal structure and releases more acid lipase; it also increases cell permeability, leading to direct contact between the enzyme and the substrate and enhancing the reaction rate (Faridnia et al., 2015). The change in neutral lipase (Fig. 1F) was slightly different in that it reached maximum activity after drying and decreased with processing time, which is consistent with the

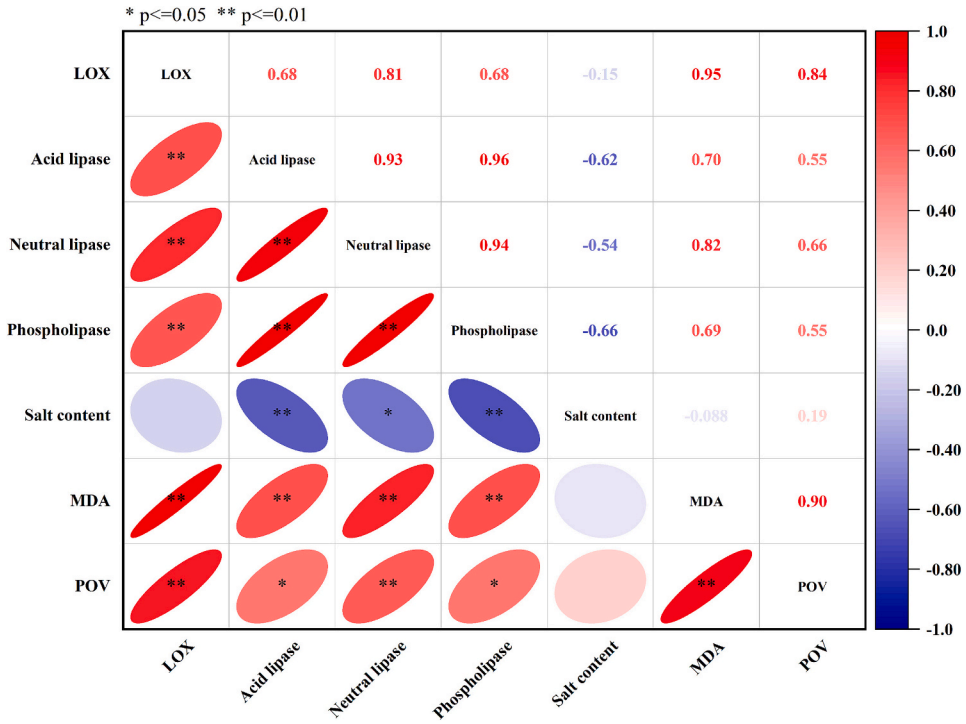

Fig. 3. Heatmap of pearson correlation analysis between basic physicochemical parameters of different treatment groups, where red colour indicates positive correlation and blue colour indicates negative correlation. Asterisks (*) indicate correlation coefficients marked as significant (*P < 0.05, **P < 0.01. (For interpretation of the references to colour in this figure legend, the reader is referred to the web version of this article.)

findings of a previous study (Liu et al., 2023). Among them, the 4-ES group showed a significant increase in neutral lipases activity by 20–46 %, which was attributed to the increased salt content in the muscle and cellular fragmentation releasing lipase after the original sodium chloride curing. The intervention of ES at this time activated more pro-enzymatic substances, which led to another enhancement of enzyme activity. The maximum post-curing activity of phospholipase (Fig. 1G) occurs because salt osmosis disrupts the cell membranes of the fat cells and phospholipase is just released from the fat tissue to participate in the hydrolysis reaction, and the addition of ES accelerates the rate of its release. At 20 day and 30 day there was a decrease in all fat hydrolase activities probable because of the increase in temperature during the maturation period when the lysosomes release proteases that are in an active phase, which have a damaging effect on fat hydrolase, which is an important reason for the decline of lipase in the later stages of the disease (Chen et al., 2023).

3.5. Correlation analysis of physicochemical properties

To thoroughly evaluate the relationships among the parameters, a correlation analysis was conducted on the basic physicochemical parameters across various treatment groups. As depicted in Fig. 3, LOX demonstrated a significant positive correlation ($p < 0.05$) with acid lipase, neutral lipase, phospholipase, MDA, and POV, and a significant negative correlation with salt content. These findings imply that the activity of LOX is correlated with the generation of lipid oxidation products, including MDA and POV (Jin et al., 2010). Furthermore, the salt content exhibited a significant negative correlation ($p < 0.05$) with acid lipase, neutral lipase, and phospholipase, as well as a positive correlation with POV. This finding implies that the salt content substantially influences the activity of several lipases. Collectively, when considered in conjunction with Fig. 1, it suggests that increased salt content may suppress enzyme activity to a certain degree (Wang et al., 2016). This study demonstrated that the ES positively influenced the enzymatic activity in dry-cured tenderloin, wherein MDA and POV, generated in the presence of the enzyme, serve as precursors for the subsequent formation of volatile compounds.

3.6. Amino acid content in dry-cured tenderloins

Amino acid constituted the fundamental units of proteins and served as key nutritional indicators and aroma compound precursors in meat quality assessment (Zhang et al., 2021). Throughout maturation, small peptides and amino acids were derived from the enzymatic breakdown of proteins, and changes in amino acids content were contingent upon the ratio between formation and degradation. The total amino acid content of dry-cured tenderloins on 1 day and 30 days of processing is shown in Fig. 4A, with a total of 15 types of amino acids detected in the samples. The total amino acid contents for the CK and 0-ES group were 212.61 mg/100 g and 159.81 mg/100 g, respectively, in the 1 day samples. For the 30 day samples, the total amino acid contents for the CK, 0-ES, 4-ES, and 11-ES groups were 628.46, 632.18, 803.26, and

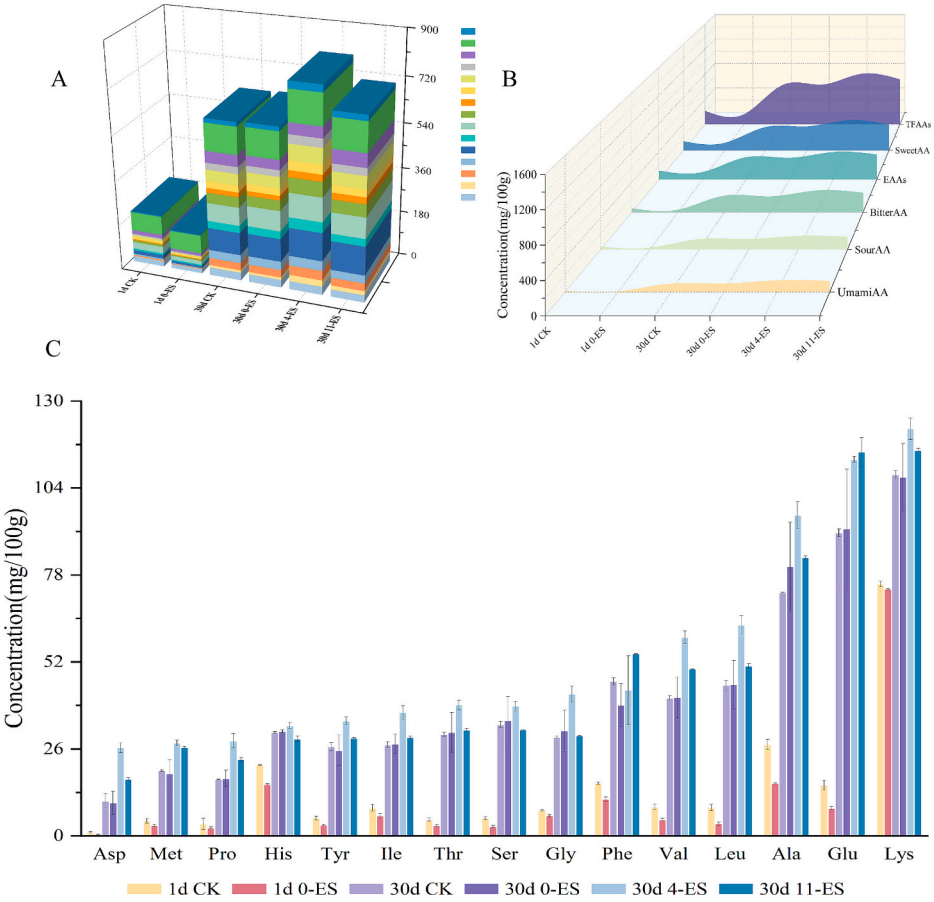

Fig. 4. Change of amino acid content.
(A) Stacked plot of changes in total FAAs content;
(B) Changes in total taste amino acid content: UmamiAA is Glu and Asp; SourAA is His, Glu and Asp; BitterAA is Phe, Leu, Ile, Tyr, Pro, Met and Val; SweetAA is Pro, Met, Val, Lys, Ala, Gly, Ser and Thr; TFAAs is the total of all the above amino acids;
(C) Histogram of changes in the content of various FAAs under different treatments.
Different lower case letters in the graphs indicate significant differences between samples at different fermentation times ($p < 0.05$).

715.65 mg/100 g, respectively. The increase in amino acid content improved the nutritional quality of dry-cured tenderloin. At 30 days, the total amino acid content of the three ES treatment groups (0-ES, 4-ES, and 11-ES) exceeded that of the CK group. This indicated that ES treatment could promote the release of amino acids; on the other hand, ES treatment also disrupted the cell membrane, leading to the release of amino acid-rich liquid (Roobab et al., 2024). The total concentrations of the various flavor amino acids in the 1 day and 30 day samples were presented in Fig. 4B. At 30 days, three ES-treated groups (0-ES, 4-ES, and 11-ES) showed a significant increase in the content of umami amino acids (umami AA), sour amino acids (sour AA), bitter amino acids (bitter AA), and sweet amino acids (sweet AA) compared to the CK group. Additionally, ES elevated essential amino acids (EAA) levels in matured samples, improving product flavor. Amino acids are key to the flavor profile in fermented tenderloin, providing distinct tastes and acting as aroma and taste compound precursors. As depicted in Fig. 4C, 15 distinct flavor amino acids were detected in the analysis of dry-cured tenderloin, with valine, leucine, alanine, glutamic acid, and lysine identified as the primary contributors to the noted increase in total amino acid content. Glutamic acid (Glu) was found to enhance umami in fermented loin and to improve the organoleptic properties of the product (Zhao et al., 2016). Alanine (Ala), conversely, was reported to positively influence umami and sweetness. Additionally, past research demonstrated that the synergistic effect between Glu-Ala and Glu-Val could elevate the intensity of fresh flavor in meat products.

3.7. Fatty acid content in dry-cured tenderloins

Fatty acids were examined in 1 day (CK, 0-ES) and 30 day (CK, 0-ES, 4-ES, 11-ES) dry-cured tenderloins, and 23 fatty acids were detected, as shown in Table 2. The fatty acid content of the dry-cured tenderloins changed slightly with increasing processing time, as did the amounts of Saturated Fatty Acids (SFAs), Monounsaturated Fatty Acids (MUFAs), and Polyunsaturated Fatty Acids (PUFAs).

In the analysis of SFAs, palmitic acid (C16:0) and stearic acid (C18:0) were identified as the predominant components. At 30 days late ripening, palmitic acid content of the ES treatment group was slightly increased compared to the CK treatment group, with 29.90 % and 29.96 % increase in palmitic acid (C16:0) content in the 4-ES and 11-ES groups, respectively (as shown in Fig. 5). The 31.44 % increase in total SFAs was attributed to its higher lipid peroxidation stabilization-ability (Chen et al., 2011).

The total MUFAs content exhibited a decline after a 30 day period, with the profile being predominantly constituted by oleic acid (C18:1n9c), as depicted in Fig. 5. Compared with the 30-day CK group, all three ES groups showed significant decreases in oleic acid content, with 29.52 % and 29.45 % decreases in the 4-ES and 11-ES groups, respectively. The reason for this is that the rate at which unsaturated oleic acid is oxidized is accelerated after ES destroys fat cells, forming aldehydes and other compounds (Rodriguez-Carpena et al., 2012).

The overall reduction in PUFA content after 30 days was predominantly attributed to linoleic acid (C18:2n6c). Linoleic acid levels exhibited a decrease of 52.61 % and 53.25 % in the 4-ES and 11-ES groups, respectively, when contrasted with the 30-day CK group (as detailed in Table 2 and illustrated in Fig. 5). Given that phospholipids, which are rich in PUFA, are inherently prone to lipid oxidation, the oxidation of phospholipid membranes was significantly enhanced following ES-induced phospholipid cell disruption. Consequently, the oxidation rate of linoleic acid and other PUFAs surpassed that of oleic acid, leading to a reduction in their content (Sun et al., 2015).

3.8. E-tongue in dry-cured tenderloins

Flavor tests were conducted on dry-cured tenderloins that had undergone ES at various time points, utilizing an e-tongue device with specialized electronic sensors. The resultant radar plot, as depicted in Fig. 6A, represents the sensorial outcomes of these tests. On the one hand, the three ES-treated groups (0-ES, 4-ES, and 11-ES) exhibited reduced levels of sourness, bitterness, astringency, aftertaste-B, andaftertaste-A. This reduction is likely attributed to the inhibition or

Table 2
Fatty acid composition of dry-cured tenderloin (1 day, 30 day).

Fatty acid (%)	1d CK	1d 0-ES	30d CK	30d 0-ES	30d 4-ES	30d 11-ES
C8:0	0.01 ± 0.000^{g}	0.01 ± 0.000^{k}	0.01 ± 0.000^{h}	0.01 ± 0.000^{h}	0.01 ± 0.000^{i}	0.01 ± 0.000^{i}
C10:0	0.06 ± 0.001^{g}	0.06 ± 0.001^{jk}	0.07 ± 0.001^{h}	0.07 ± 0.002^{h}	0.58 ± 0.022^{gh}	0.59 ± 0.024^{gh}
C12:0	0.08 ± 0.003^{g}	0.08 ± 0.002^{ijk}	0.08 ± 0.001^{h}	0.08 ± 0.003^{h}	0.08 ± 0.003^{i}	0.08 ± 0.003^{i}
C14:0	1.28 ± 0.044^{e}	1.29 ± 0.022^{f}	1.29 ± 0.033^{f}	1.30 ± 0.043^{f}	1.29 ± 0.046^{f}	1.29 ± 0.048^{f}
C14:1n5	0.01 ± 0.000^{g}	0.01 ± 0.000^{k}	0.01 ± 0.000^{h}	0.01 ± 0.000^{h}	0.01 ± 0.000^{i}	0.01 ± 0.000^{i}
C15:0	0.04 ± 0.001^{g}	0.04 ± 0.000^{k}	0.04 ± 0.001^{h}	0.04 ± 0.001^{h}	0.04 ± 0.001^{i}	0.04 ± 0.001^{i}
C16:0	24.6 ± 0.465^{b}	18.67 ± 0.244^{b}	21.73 ± 0.336^{b}	22.32 ± 0.124^{b}	29.90 ± 0.689^{a}	29.96 ± 0.738^{a}
C16:1n7	1.51 ± 0.018^{e}	14.84 ± 0.153^{c}	14.82 ± 0.173^{c}	15.04 ± 0.233^{c}	14.82 ± 0.164^{c}	14.90 ± 0.251^{c}
C17:0	0.23 ± 0.008^{f}	0.23 ± 0.007^{h}	0.23 ± 0.007^{h}	0.23 ± 0.008^{h}	0.23 ± 0.008^{hi}	0.23 ± 0.008^{hi}
C18:0	13.33 ± 0.096^{d}	13.17 ± 0.012^{d}	10.79 ± 0.032^{e}	13.33 ± 0.194^{e}	13.17 ± 0.134^{d}	13.14 ± 0.122^{d}
C18:1n9t	0.11 ± 0.003^{g}	0.11 ± 0.003^{hijk}	0.11 ± 0.003^{h}	0.11 ± 0.004^{h}	0.11 ± 0.004^{i}	0.11 ± 0.004^{i}
C18:1n9c	39.86 ± 1.110^{a}	37.47 ± 0.071^{a}	35.53 ± 0.461^{a}	30.58 ± 0.486^{a}	29.52 ± 0.670^{b}	29.45 ± 0.671^{b}
C18:2n6c	16.26 ± 0.121^{c}	11.22 ± 0.233^{e}	12.47 ± 0.216^{d}	13.7 ± 0.425^{d}	6.56 ± 0.221^{e}	6.64 ± 0.111^{e}
C20:0	0.20 ± 0.003^{g}	0.20 ± 0.006^{hij}	0.19 ± 0.000^{h}	0.20 ± 0.007^{h}	0.19 ± 0.005^{i}	0.19 ± 0.003^{i}
C18:3n6	0.03 ± 0.000^{g}	0.03 ± 0.000^{k}	0.03 ± 0.000^{h}	0.03 ± 0.002^{h}	0.03 ± 0.001^{i}	0.03 ± 0.001^{i}
Fatty acid (%)	1d CK	1d 0-ES	30d CK	30d 0-ES	30d 4-ES	30d 11-ES
C18:3n3	0.83 ± 0.015^{g}	0.82 ± 0.026^{g}	0.83 ± 0.024^{g}	0.85 ± 0.028^{g}	0.91 ± 0.027^{g}	0.89 ± 0.028^{g}
C20:1	0.78 ± 0.003^{f}	0.77 ± 0.022^{g}	0.78 ± 0.015^{g}	0.80 ± 0.027^{g}	0.77 ± 0.028^{g}	0.78 ± 0.026^{g}
C20:2	0.72 ± 0.005^{f}	0.72 ± 0.017^{g}	0.72 ± 0.013^{g}	0.73 ± 0.040^{g}	0.72 ± 0.004^{g}	0.72 ± 0.026^{g}
C22:0	0.03 ± 0.000^{g}	0.03 ± 0.000^{k}	0.03 ± 0.000^{h}	0.03 ± 0.001^{h}	0.03 ± 0.000^{i}	0.03 ± 0.002^{i}
C20:3n6	0.09 ± 0.001^{g}	0.09 ± 0.003^{hijk}	0.09 ± 0.001^{h}	0.09 ± 0.004^{h}	0.09 ± 0.003^{i}	0.09 ± 0.003^{i}
C22:1n9	0.14 ± 0.003^{g}	0.14 ± 0.003^{hijk}	0.14 ± 0.002^{h}	0.14 ± 0.005^{h}	0.21 ± 0.003^{hi}	0.21 ± 0.005^{hi}
C20:4n6	0.21 ± 0.006^{g}	0.21 ± 0.006^{hi}	0.21 ± 0.003^{h}	0.21 ± 0.006^{h}	0.33 ± 0.012^{hi}	0.33 ± 0.012^{hi}
C22:6n3	0.02 ± 0.000^{g}	0.02 ± 0.001^{k}	0.02 ± 0.000^{h}	0.02 ± 0.001^{h}	0.03 ± 0.001^{i}	0.03 ± 0.001^{i}
SFA	40.53 ± 0.627^{b}	34.47 ± 0.311^{d}	35.15 ± 0.424^{d}	38.31 ± 0.422^{c}	46.21 ± 0.912^{a}	46.26 ± 0.974^{a}
MUFA	42.28 ± 1.133^{d}	53.20 ± 0.249^{a}	51.25 ± 0.651^{b}	46.54 ± 0.750^{c}	45.23 ± 0.867^{c}	45.25 ± 0.953^{c}
PUFA	17.62 ± 0.147^{a}	12.57 ± 0.271^{d}	13.82 ± 0.247^{c}	15.07 ± 0.472^{b}	8.19 ± 0.268^{e}	8.25 ± 0.162^{e}

SFA denotes saturated fatty acids, MUFA denotes monounsaturated fatty acids, and PUFA denotes polyunsaturated fatty acids. All data in the table indicate the proportion of each fatty acid in the total fatty acid composition in %, different lower case letters in the same row indicate significant differences in fatty acid content between groups ($p < 0.05$).

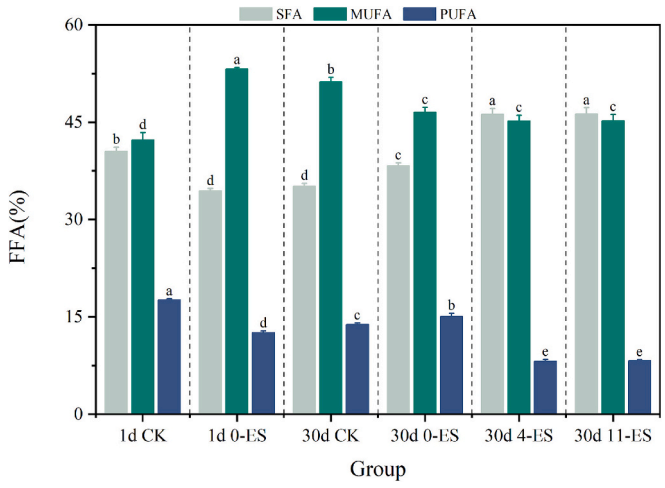

Fig. 5. Changes in the contents of saturated fatty acids (SFA), monounsaturated fatty acids (MUFA) and polyunsaturated fatty acids (PUFA). Different lower case letters indicate differences between samples ($p < 0.05$).

destruction of intermediate flavor compounds by ES treatment, potentially enhanced by the presence of higher salt levels (Zhang et al., 2024). The levels of umami, richness, and saltiness increased in all three groups: 0-ES, 4-ES, and 11-ES. The increase was due to the accelerated breakdown of tenderloin proteins into umami-rich amino acids, enhanced by NaCl and ES, and their accumulation during ripening. Specifically, the 4-ES and 11-ES groups showed heightened umami, richness, and saltiness, likely due to salt's cellular disruption, ES-enhanced oxidation, and improved salt diffusion. The PCA analysis, depicted in Fig. 6B, presents a more intuitive visualization of the flavor differences identified by the e-tongue. In this context, PC1 and PC2 are responsible for 73.0 % and 19.0 % of the variance, respectively. As shown in Fig. 6B, together they account for 92.0 % (surpassing the 85 %) of the total variance, which suggests that the data has a high degree of reproducibility.

3.9. E-nose in dry-cured tenderloins

An e-nose mimics the human nose's olfactory system, identifying various molecules through an array of sensors sensitive to minor changes in volatile organic compounds. The radar plots (Fig. 6C) of dry-cured tenderloins treated with ES at different periods showed significant sensor response differences ($p < 0.05$). The results show the e-nose can distinguish dry-cured tenderloin samples treated with ES at various times. Sensors W1S, W1W, W2S, and W2W had higher responses, suggesting key compounds like methyl groups, sulphides, and aromatics are major contributors to the tenderloin's flavor. This aligns with our team's past findings, confirming the e-nose's ability to discern tenderloin flavors (Tian et al., 2022). In the 4-ES group, sensors W1S, W1W, and W2W had the highest responses, significantly exceeding the CK. This suggests that fermentation in dry-cured tenderloin led to the release of volatiles like methyl groups and sulphides from lipids, proteins, and carbohydrates. Moreover, ES treatment boosted flavor-related sensor responses in all groups, enhancing the tenderloin's flavor profile. Principal component (PC) analysis was used to resolve the changes in aroma of dry-cured tenderloin treated with ES at different times, and the results are shown in Fig. 6D: grey (CK), green (0-ES), red (4-ES) and blue (11-

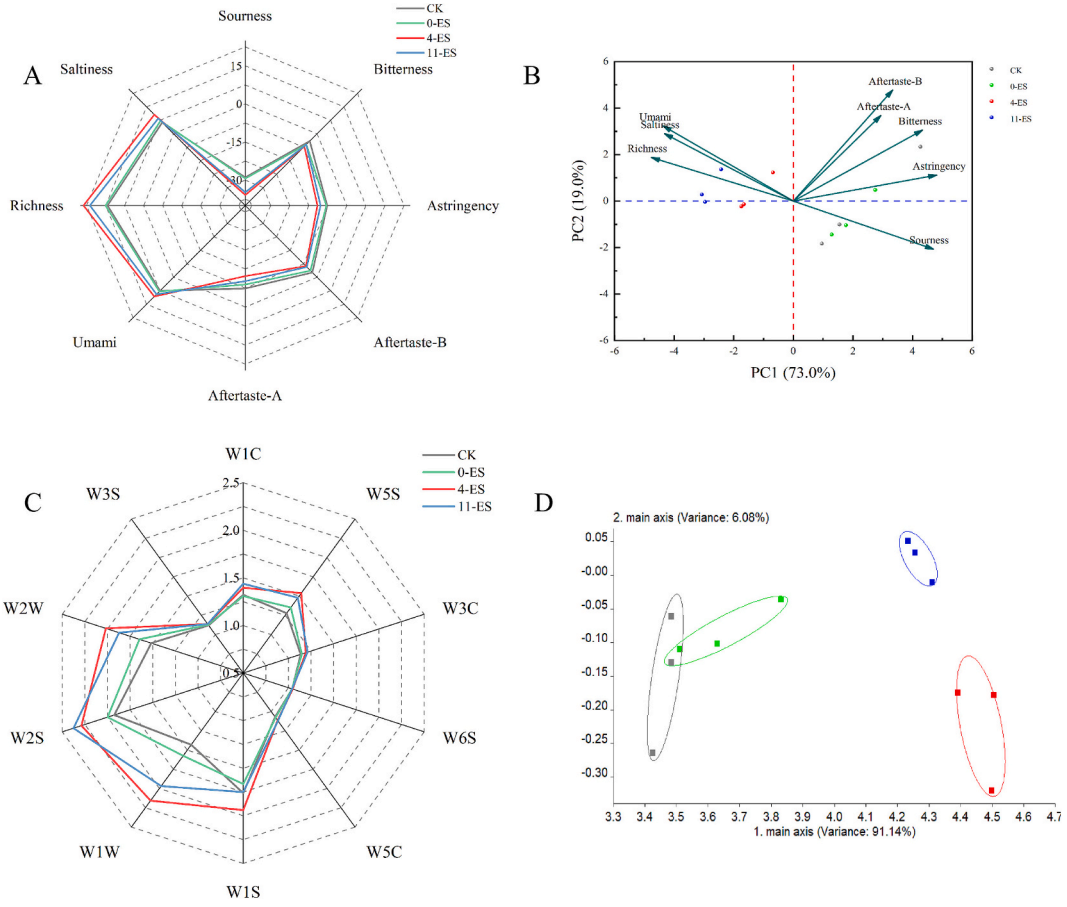

Fig. 6. Radar plot of e-tongue taste values (A); principal component analysis plot (B); radar plot of e-nose aroma values (C) and principal component analysis plot (D).

ES). PC1 and PC2 explained 91.14 % and 6.08 % of the variance, respectively, totaling 97.22 %. This high cumulative variance suggests that the principal components fully captured the odor profile of ES-treated dry-cured tenderloin, as only contributions over 85 % are considered representative (Liu et al., 2018). Fig. 6D illustrates significant variations in aroma distributions among dry-cured tenderloin treatment groups, reflecting substantial differences in volatile compounds. Differences between the CK and ES-treated groups are due to changes in volatile compounds resulting from lipid oxidation and secondary product formation, along with other biochemical reactions. We postulate that dry-cured tenderloins treated with ES after marination and drying might produce unique flavor compounds that boost sensor responses, possibly due to a synergistic "stacking effect" between NaCl and ES.

3.10. Volatile organic compounds in dry-cured tenderloins

The volatile flavor compounds that had been produced from dry-cured tenderloins were attributed to chemical reactions involving various flavor precursors. Among these, the Maillard reaction and lipid oxidative degradation were identified as key processes in the generation of VOCs (Zhang et al., 2023). Table 3 displayed that 49 volatile compounds were identified in the dry-cured tenderloin at 30 days, which were categorized into 6 categories: 8 alcohols, 11 aldehydes, 7 esters, 7 ketones, 6 alkanes, and 10 other compounds. In the different treatment groups, 27, 33, 48, and 38 compounds were detected in the A (CK), B (0-ES), C (4-ES), and D (11-ES) groups, respectively. This suggested that the use of ES at the intermediate stage of processing was more effective in promoting the production of flavor compounds than the use of ES at the beginning of processing, thus potentially enhancing the overall flavor of dry-cured tenderloin.

Upon integrating the comparative heat map depicting variations in the volatile compound profiles across distinct sample groups (Fig. 7), it became evident that aldehyde levels peaked in groups A (CK) and B (0-ES), attributed to their heightened sensitivity at lower detection limits. In the analysis, the most prominent concentrations were identified for 2-

Table 3
Changes in the types and relative contents of volatile flavor compounds in dry-cured tenderloin after ES treatment at different times.

class	Name of compound	CAS	Group (relative content %)			
			CK	0-ES	4-ES	11-ES
Alcohols	1-octanol	111–87-5	1.05	0.87	0.93	1.16
	4-ethylcyclohexanol	4534-74-1	0.65	0.33	2.04	0.98
	cyclohexanol, 1-methyl-4-(1-methylethyl)	21,129–27-1	–	–	1.00	–
	ethanol	64–17-5	1.00	1.11	0.99	0.91
	isoamyl alcohol	123–51-3	0.73	0.83	0.85	0.93
	linalool	78–70-6	–	–	0.67	–
	n-pentyl alcohol	71–41-0	1.58	1.26	0.40	0.43
	n-propanol	71–23-8	0.54	–	0.89	0.91
Aldehydes	2-methyl-2-butenal	1115-11-3	1.11	0.87	0.59	0.43
	2-methylbutyraldehyde	96–17-3	0.86	1.08	1.04	1.03
	3-methylbutanal	590–86-3	0.92	1.03	1.05	1.00
	4-propylbenzaldehyde	28,785–06-0	–	0.41	1.12	1.14
	9-octadecenal	5090-41-5	–	1.15	0.89	0.63
	decaldehyde	112–31-2	0.58	–	–	1.42
	hexaldehyde	66–25-1	1.75	1.37	0.29	0.59
	lauryl aldehyde	112–54-9	1.09	0.67	0.97	0.94
	n-heptanal	111–71-7	1.33	0.97	0.15	1.21
	nonanal	124–19-6	1.14	0.96	0.83	1.07
	octadecanal	638–66-4	1.07	1.08	1.12	0.73
Alkanes	2-methylundecane	7045-71-8	–	–	1.21	0.79
	4,8-dimethylundecane	17,301–33-6	–	–	1.00	–
	propylcyclopropane	2415-72-7	–	–	0.67	–
	n-decane	124–18-5	0.25	1.04	1.38	1.32
	n-octane	111–65-9	0.66	1.29	0.98	1.08
	n-tetradecane	629–59-4	–	0.76	1.81	0.44
Esters	ethyl 2-ethylhexanoate	2983-37-1	0.10	0.38	1.15	2.03
	ethyl acetate	141–78-6	0.25	0.88	0.98	1.89
	ethyl caprate	110–38-3	–	–	1.01	0.99
	ethyl lactate	97–64-3	–	–	0.47	1.20
	ethyl myristate	124–06-1	–	0.23	1.83	0.61
	ethyl palmitate	628–97-7	0.15	0.48	2.26	1.11
	ethyl 9-hexadecenoate	54,546–22-4	–	–	1.34	0.66
Ketones	2,3-octanedione	585–25-1	–	–	0.73	0.94
	2-octanone	111–13-7	0.84	0.74	1.14	0.94
	3-octanone	106–68-3	0.87	0.93	1.20	–
	cyclohexanone	108–94-1	–	–	0.90	0.77
	diacetyl	431–03-8	–	–	0.55	0.78
	geranylacetone	3796-70-1	–	–	0.67	–
	isomenthone	491–07-6	–	–	0.67	–
Others	1,4-dichlorobenzene	106–46-7	0.59	0.84	1.13	1.44
	2-ethyl-1-octene	51,655–64-2	–	0.88	0.78	–
	trans-2-octene	13,389–42-9	–	–	1.00	–
	(*R*)-4-Methylhexanoic acid	52,745–93-4	–	0.63	1.09	1.28
	benzene	71–43-2	–	0.12	1.55	–
	ethylbenzene	100–41-4	0.63	1.50	0.89	0.98
	methyl diethyldithiocarbamate	686–07-7	–	0.23	1.61	0.83
	myrcene	123–35-3	0.37	0.44	1.52	–
	p-cresol	106–44-5	0.34	0.52	1.78	1.03
	phenol	108–95-2	0.15	0.10	3.29	0.46

Note: Results are expressed as the average of 3 replicates for each sample. "-" means that the compound was not detected.

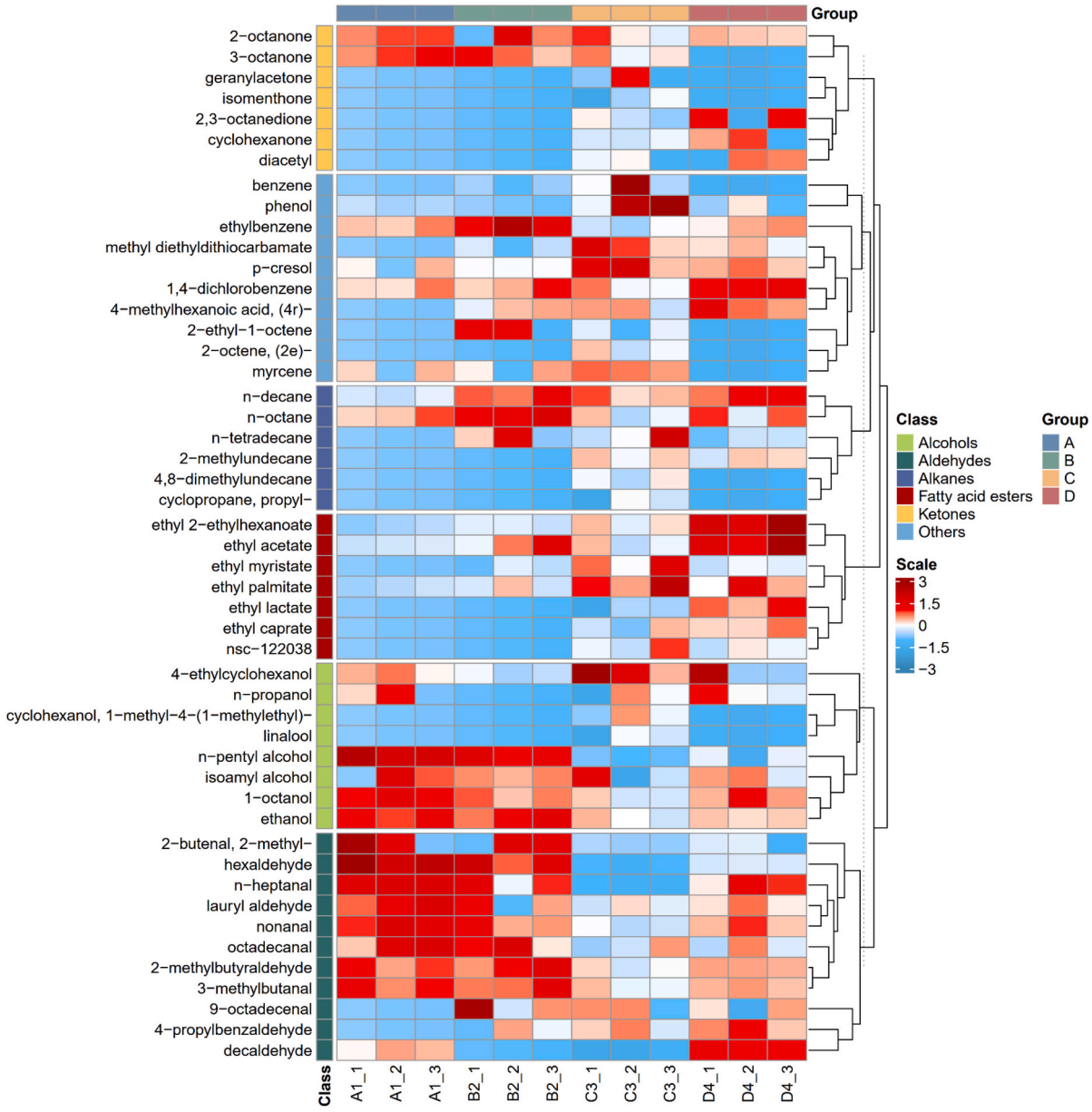

Fig. 7. GC–MS to detect changes in volatile components after different times of ES treatment. A (CK group), B (0-ES group), C (4-ES group), and D (11-ES group) in the heat map. Three parallel samples were detected for each treatment group.

methyl-2-butenal, hexanal, laural, heptanal, and nonanal. Elevated concentrations of aldehydes due to lipid peroxidation were one of the reasons for the presence of characteristic fatty and herbaceous odors in meat products, which were found to originate mainly from the oxidative degradation of polyunsaturated fatty acids (Saldaña et al., 2019). However, previous research indicated that an elevated level of hexanal could confer an undesirable, rancid odor to the ham, hence, the observed decrease in hexanal in groups C (4-ES) and D (11-ES) was advantageous for enhancing the overall sensory profile of the dry-cured tenderloin. In the study, 1-octanol, ethanol, and n-pentanol were identified as the predominant alcohols, predominantly observed in group A (CK). However, group C (4-ES) exhibited the highest count of additional alcohols, notably α,α-4-trimethylcyclohexanemethanol and linalool, which were exclusively identified within this group. This observation suggests that their presence might be attributed to the synergistic influence of NaCl and ES. In the analysis, 7 esters were identified in the samples using GC–MS. These esters were predominantly formed through the esterification of alcohols and acids present in the meat products, and were reported to confer a sweet and fruity taste (Han et al., 2024). Ethyl caprate, ethyl lactate, ethyl myristate, and ethyl 9-hexadecenoate were specifically identified in the experimental groups subjected to ES treatment (B, C, and D), with group C exhibiting the highest concentrations of these compounds. ES catalyzed the esterification of alcohols and acids to produce unique esters that enhanced the flavor of dry-cured tenderloins. It was demonstrated that ketones significantly contributed to the aroma of meat products and that they conveyed a rich spectrum of specific flavors (Zhang et al., 2018). Intriguingly, in the analysis of ketones, 7 were identified in the samples; however, 5, namely 2,3-octanedione, cyclohexanone, diacetyl, geranylacetone, and isomentamide, were exclusively found in groups C (4-ES) and D (11-ES), and among these, geranylacetone and isomentamide were uniquely present in group C (4-ES). The analysis indicated that ES treatment following a 4-day salt curing period facilitated the generation of specific ketones, thereby enhancing the flavor profile of dry-cured tenderloin. Despite the detection of various alkanes across all treatment groups, their contribution to the overall flavor was minimal owing to higher perceptual

thresholds, and further investigation into their biosynthetic origins and underlying mechanisms was warranted.

4. Conclusions

The objective of this study was to assess the impact of ES at various stages of dry-cured tenderloin processing. The results showed that ES promoted salt diffusion and cellular disruption and increased lipase and LOX activities, as indicated by increased levels of the lipid oxidation products MDA and POV. ES doubled the total FAA content, increased the content of SFA, and reduced the contents of MUFA and PUFA. Additionally, ES intensified the sensations of saltiness, umami, and richness, while mitigating sour, bitter, and astringent tastes, and augmented the electronic nose response values for W5S, W1S, W1W, and W2W compounds. Among the 49 compounds identified by GC–MS, ES not only heightened compound concentrations but also uniquely detected certain compounds. In conclusion, this study pioneers the exploration of ES as a potential tool for enhancing enzyme activity and flavor quality during the deep processing of meat products, opening new avenues for improving product characteristics.

CRediT authorship contribution statement

Lisha Lan: Writing – original draft, Visualization, Validation, Software, Resources, Project administration, Methodology, Investigation, Formal analysis, Data curation. **Li Chen:** Writing – review & editing, Supervision, Investigation. **Xiaolin Zhong:** Writing – review & editing, Supervision, Investigation. **Weiguo Cao:** Writing – review & editing, Supervision, Investigation. **Ying Zhou:** Writing – review & editing, Supervision, Conceptualization. **Jing Wan:** Writing – review & editing, Supervision, Conceptualization. **Yuanyuan Liu:** Writing – review & editing, Supervision, Conceptualization. **Qinjin Zhu:** Writing – review & editing, Supervision, Project administration, Funding acquisition, Conceptualization.

Declaration of competing interest

The authors declare that they have no known competing financial interests or personal relationships that could have appeared to influence the work reported in this paper.

Acknowledgments

This study was funding by the National Natural Science Foundation Project, China (No. 32272359).

Appendix A. Supplementary data

Supplementary data to this article can be found online at https://doi.org/10.1016/j.fochx.2025.102189.

Data availability

Data will be made available on request.

References

Cao, Q., Du, H., Huang, Y., Hu, Y., You, J., Liu, R., … Manyande, A. (2019). The inhibitory effect of chlorogenic acid on lipid oxidation of grass carp (Ctenopharyngodon idellus) during chilled storage. *Food and Bioprocess Technology, 12*(12), 2050–2061. https://doi.org/10.1007/s11947-019-02365-0

Chaves Almeida, F. L., Silveira, M. P., Alvim, I. D., da Costa, T. B., da Silva, T. L., Adeodato Vieira, M. G., … Soares Forte, M. B. (2023). Jet cutter technique as a tool to achieve high lipase hydrolytic activity. *Food and Bioproducts Processing, 137*, 189–199. https://doi.org/10.1016/j.fbp.2022.12.001

Chen, B., McClements, D. J., & Decker, E. A. (2011). Minor components in food oils: A critical review of their roles on lipid oxidation Chemistry in bulk oils and emulsions. *Critical Reviews in Food Science and Nutrition, 51*(10), 901–916. https://doi.org/10.1080/10408398.2011.606379

Chen, C., Fan, X., Hu, Y., Zhou, C., Sun, Y., Du, L., & Pan, D. (2023). Effect of different salt substitutions on the decomposition of lipids and volatile flavor compounds in restructured duck ham. *Lwt-Food SCIENCE and Technology, 176*. https://doi.org/10.1016/j.lwt.2023.114541

Chen, J., Zhang, L., Guo, X., Qiang, J., Cao, Y., Zhang, S., & Yu, X. (2024). Influence of triacylglycerol structure on the formation of lipid oxidation products in different vegetable oils during frying process. *Food Chemistry, 464*(Pt 1), 141783. https://doi.org/10.1016/j.foodchem.2024.141783

Contreras-Lopez, G., Carnero-Hernandez, A., Huerta-Jimenez, M., Delia Alarcon-Rojo, A., Garcia-Galicia, I., & Carrillo-Lopez, L. M. (2020). High-intensity ultrasound applied on cured pork: Sensory and physicochemical characteristics. *Food Science & Nutrition, 8*(2), 786–795. https://doi.org/10.1002/fsn3.1321

Dias, A. L. B., dos Santos, P., & Martínez, J. (2018). Supercritical CO2 technology applied to the production of flavor ester compounds through lipase-catalyzed reaction: A review. *Journal of CO_2 Utilization, 23*, 159–178. https://doi.org/10.1016/j.jcou.2017.11.011

Du, H., Chen, Q., Liu, Q., Wang, Y., & Kong, B. (2021). Evaluation of flavor characteristics of bacon smoked with different woodchips by HS-SPME-GC-MS combined with an electronic tongue and electronic nose. *Meat Science, 182*. https://doi.org/10.1016/j.meatsci.2021.108626

Faridnia, F., Ma, Q. L., Bremer, P. J., Burritt, D. J., Hamid, N., & Oey, I. (2015). Effect of freezing as pre-treatment prior to pulsed electric field processing on quality traits of beef muscles. *Innovative Food Science & Emerging Technologies, 29*, 31–40. https://doi.org/10.1016/j.ifset.2014.09.007

Fernandez, M., Hospital, X. F., Cabellos, C., & Hierro, E. (2020). Effect of pulsed light treatment on Listeria inactivation, sensory quality and oxidation in two varieties of Spanish dry-cured ham. *Food Chemistry, 316*. https://doi.org/10.1016/j.foodchem.2020.126294

Fu, Y., Cao, S., Yang, L., & Li, Z. (2022). Flavor formation based on lipid in meat and meat products: A review. *Journal of Food Biochemistry, 46*(12). https://doi.org/10.1111/jfbc.14439

Guo, X., Lu, S., Wang, Y., Dong, J., Ji, H., & Wang, Q. (2019). Correlations among flavor compounds, lipid oxidation indices, and endogenous enzyme activity during the processing of Xinjiang dry-cured mutton ham. *Journal of Food Processing and Preservation, 43*(11). https://doi.org/10.1111/jfpp.14199

Han, S., Ke, M., Wang, L., Ma, H., Wu, G., Zhu, L., … Lu, H. (2024). Identification of dynamic changes in volatile compounds and metabolites during the smoking process of Zhenba bacon by GC-IMS combined metabolomics. *Food Research International, 182*. https://doi.org/10.1016/j.foodres.2024.114197

Hu, S. Q., Xu, X. L., Zhang, W. A., Li, C. B., & Zhou, G. H. (2023). Controlling cathepsin B activity in Jinhua ham through multifactorial analysis and modeling of temperature, pH and salt content. *Food Control, 154*. https://doi.org/10.1016/j.foodcont.2023.109974

Hwang, I. H., Devine, C. E., & Hopkins, D. L. (2003). The biochemical and physical effects of electrical stimulation on beef and sheep meat tenderness. *Meat Science, 65*(2), 677–691. https://doi.org/10.1016/s0309-1740(02)00271-1

Jin, G., Zhang, J., Yu, X., Zhang, Y., Lei, Y., & Wang, J. (2010). Lipolysis and lipid oxidation in bacon during curing and drying-ripening. *Food Chemistry, 123*(2), 465–471. https://doi.org/10.1016/j.foodchem.2010.05.031

Karabagias, I., Badeka, A., & Kontominas, M. G. (2011). Shelf life extension of lamb meat using thyme or oregano essential oils and modified atmosphere packaging. *Meat Science, 88*(1), 109–116. https://doi.org/10.1016/j.meatsci.2010.12.010

Lapenna, D., Ciofani, G., Pierdomenico, S. D., Neri, M., Cuccurullo, C., Giamberardino, M. A., & Cuccurullo, F. (2009). Inhibitory activity of salicylic acid on lipoxygenase-dependent lipid peroxidation. *Biochimica et Biophysica Acta-General Subjects, 1790*(1), 25–30. https://doi.org/10.1016/j.bbagen.2008.09.007

Liu, J., Shen, S., Xiao, N., Jiang, Q., & Shi, W. (2022). Effect of glycation on physicochemical properties and volatile flavor characteristics of silver carp mince. *Food Chemistry, 386*. https://doi.org/10.1016/j.foodchem.2022.132741

Liu, Q., Zhao, N., Zhou, D., Sun, Y., Sun, K., Pan, L., & Tu, K. (2018). Discrimination and growth tracking of fungi contamination in peaches using electronic nose. *Food Chemistry, 262*, 226–234. https://doi.org/10.1016/j.foodchem.2018.04.100

Liu, X., Piao, C., Ju, M., Zhang, J., Zhang, W., Cui, F., … Cui, M. (2023). Effects of low salt on lipid oxidation and hydrolysis, fatty acids composition and volatiles flavor compounds of dry-cured ham during ripening. *Lwt-Food Science and Technology, 187*. https://doi.org/10.1016/j.lwt.2023.115347

Lorido, L., Estévez, M., Ventanas, J., & Ventanas, S. (2015). Salt and intramuscular fat modulate dynamic perception of flavour and texture in dry-cured hams. *Meat Science, 107*, 39–48. https://doi.org/10.1016/j.meatsci.2015.03.025

Ma, H. J., Ledward, D. A., Zamri, A. I., Frazier, R. A., & Zhou, G. H. (2007). Effects of high pressure/thermal treatment on lipid oxidation in beef and chicken muscle. *Food Chemistry, 104*(4), 1575–1579. https://doi.org/10.1016/j.foodchem.2007.03.006

Martuscelli, M., Lupieri, L., Sacchetti, G., Mastrocola, D., & Pittia, P. (2017). Prediction of the salt content from water activity analysis in dry-cured ham. *Journal of Food Engineering, 200*, 29–39. https://doi.org/10.1016/j.jfoodeng.2016.12.017

Ripolles, S., Bastianello Campagnol, P. C., Armenteros, M., Aristoy, M. C., & Toldra, F. (2011). Influence of partial replacement of NaCl with KCl, CaCl2 and MgCl2 on lipolysis and lipid oxidation in dry-cured ham. *Meat Science, 89*(1), 58–64. https://doi.org/10.1016/j.meatsci.2011.03.021

Rodriguez-Carpena, J. G., Morcuende, D., & Estevez, M. (2012). Avocado, sunflower and olive oils as replacers of pork back-fat in burger patties: Effect on lipid composition, oxidative stability and quality traits. *Meat Science, 90*(1), 106–115. https://doi.org/10.1016/j.meatsci.2011.06.007

Roobab, U., Chen, B.-R., Madni, G. M., Tong, Z. G., Zeng, X.-A., Abdi, G., … Aadil, R. M. (2024). Evaluation of ultrasound and pulsed electric field combinations on the cooking losses, texture profile, and taste-related amino acids of chicken breast meat. *Ultrasonics Sonochemistry, 107*. https://doi.org/10.1016/j.ultsonch.2024.106919

Saldaña, E., Saldarriaga, L., Cabrera, J., Siche, R., Behrens, J. H., Selani, M. M., … Contreras-Castillo, C. J. (2019). Relationship between volatile compounds and consumer-based sensory characteristics of bacon smoked with different Brazilian woods. *Food Research International, 119*, 839–849. https://doi.org/10.1016/j.foodres.2018.10.067

Sun, H. X., Zhong, R. Z., Liu, H. W., Wang, M. L., Sun, J. Y., & Zhou, D. W. (2015). Meat quality, fatty acid composition of tissue and gastrointestinal content, and antioxidant status of lamb fed seed of a halophyte (Suaeda glauca). *Meat Science, 100*, 10–16. https://doi.org/10.1016/j.meatsci.2014.09.005

Tian, Z., Zhu, Q., Chen, Y., Zhou, Y., Hu, K., Li, H., … Chen, X. (2022). Studies on flavor compounds and free amino acid dynamic characteristics of fermented pork loin ham with a complex starter. *Foods, 11*(10). https://doi.org/10.3390/foods11101501

Wang, Y., Jiang, Y.-T., Cao, J.-X., Chen, Y.-J., Sun, Y.-Y., Zeng, X.-Q., … Gan, N. (2016). Study on lipolysis-oxidation and volatile flavour compounds of dry-cured goose with different curing salt content during production. *Food Chemistry, 190*, 33–40. https://doi.org/10.1016/j.foodchem.2015.05.048

Xu, A., Chang, R., & Zhu, Q. (2022). Effect of electrical stimulation on red meat Neu5Gc content reduction: A combined experimental and DFT study. *Food Science and Human Wellness, 11*(4), 982–991. https://doi.org/10.1016/j.fshw.2022.03.023

Yue, X., Bi, S., Li, X., Zhang, X., Lan, L., Chen, L., … Zhu, Q. (2024). Electrical stimulation induces activation of mitochondrial apoptotic pathway and Down-regulates heat shock proteins in pork: An innovative strategy for enhancing the ripening process and quality of dry-cured loin ham. *Foods, 13*(11). https://doi.org/10.3390/foods13111717

Zhang, L., Yin, M. Y., & Wang, X. C. (2021). Meat texture, muscle histochemistry and protein composition of Eriocheir sinensis with different size traits. *Food Chemistry, 338*. https://doi.org/10.1016/j.foodchem.2020.127632

Zhang, M., Chen, X., Hayat, K., Duhoranimana, E., Zhang, X., Xia, S., … Xing, F. (2018). Characterization of odor-active compounds of chicken broth and improved flavor by thermal modulation in electrical stewpots. *Food Research International, 109*, 72–81. https://doi.org/10.1016/j.foodres.2018.04.036

Zhang, X., Bi, S., Li, M., Yue, X., Wan, J., Zhou, Y., … Zhu, Q. (2024). Study on activation strategy and effect of protease activity during the post-processing stage of dry-cured meat based on electrical stimulation. *Food Control, 161*. https://doi.org/10.1016/j.foodcont.2024.110363

Zhang, Y., Ji, X., Mao, Y., Luo, X., Zhu, L., & Hopkins, D. L. (2019). Effect of new generation medium voltage electrical stimulation on the meat quality of beef slaughtered in a Chinese abattoir. *Meat Science, 149*, 47–54. https://doi.org/10.1016/j.meatsci.2018.11.011

Zhang, Z., Wu, Y., Liu, Q., Zhao, G., Wei, L., Zhang, C., & Huang, F. (2023). Comparative flavor precursors and volatile compounds of Wenchang chickens fed with copra meal based on GC–O–MS. *Food Research International, 174*. https://doi.org/10.1016/j.foodres.2023.113646

Zhao, C. J., Schieber, A., & Gaenzle, M. G. (2016). Formation of taste-active amino acids, amino acid derivatives and peptides in food fermentations - a review. *Food Research International, 89*, 39–47. https://doi.org/10.1016/j.foodres.2016.08.042